Inorganic Chemistry
Article

Inorg. Chem. **2011**, *50*, 489–502 **489**
DOI: 10.1021/ic1013768

From Thioxo Cluster to Dithio Cluster: Exploring the Chemistry of Polynuclear Zirconium Complexes with S,O and S,S Ligands

Federica Maratini,[†] Luciano Pandolfo,*[,†] Maria Bendova,[‡] Ulrich Schubert,[‡] Matthias Bauer,[§] Massimiliano Rocchia,[⊥] Alfonso Venzo,[○,†] Eugenio Tondello,[○,†] and Silvia Gross*[,○,†]

[†]*Dipartimento di Scienze Chimiche, Università degli Studi di Padova, via Marzolo 1, I-35131 Padova, Italy,* [‡]*Institut für Materialchemie, Technische Universität Wien, Getreidemarkt 9, A-1060 Vienna, Austria,* [§]*Institut für Technische Chemie und Polymerchemie, Karlsruhe Institute of Technology, Engesserstrasse 18, D-76128 Karlsruhe, Germany,* [⊥]*Thermo Fisher Scientific, strada Rivoltana, I-20090 Milan, Italy, and* [○]*Istituto di Scienze e Tecnologie Molecolari, CNR-ISTM, Consiglio Nazionale delle Ricerche, and INSTM, UdR Padova, via Marzolo 1, I-35131 Padova, Italy*

Received July 10, 2010

Three different zirconium thio and oxothio clusters, characterized by different coordination modes of dithioacetate and/or monothioacetate ligands, were obtained by the reaction of monothioacetic acid with zirconium *n*-butoxide, $Zr(O^nBu)_4$, in different experimental conditions. In particular, we isolated the three polynuclear $Zr_3(\mu_3\text{-}SSSCCH_3)_2(SSCCH_3)_6\cdot 2^nBuOH$ (**Zr_3**), $Zr_4(\mu_3\text{-}O)_2(\mu\text{-}\eta^1\text{-}SOCCH_3)_2(SOCCH_3)_8(O^nBu)_2$ (**Zr_4**), and $Zr_6(\mu_3\text{-}O)_5(\mu\text{-}SOCCH_3)_2(\mu\text{-}OOCCH_3)(SOCCH_3)_{11}(^nBuOH)$ (**Zr_6**) derivatives, presenting some peculiar characteristics. **Zr_6** has an unusual star-shaped structure. Only sulfur-based ligands, viz., chelating dithioacetate monoanions and an unusual ethane-1,1,1-trithiolate group μ_3 coordinating the Zr ions, were observed in the case of **Zr_3**. 1D and 2D NMR analyses confirmed the presence of differently coordinated ligands. Raman spectroscopy was further used to characterize the new polynuclear complexes. Time-resolved extended X-ray absorption fine structure measurements, devoted to unraveling the cluster formation mechanisms, evidenced a fast coordination of sulfur ligands and subsequent relatively rapid rearrangements.

1. Introduction

The sulfur chemistry of transition metals represents a challenging and exciting research topic in the field of inorganic and structural chemistry, which has actually been thoroughly explored by several authors.[1]

Because of the peculiar features of sulfur species, such as high polarizability, large negative charge, coordination versatility, and manifold apticity, sulfur-based ligands often present a "chameleonic" behavior with respect to their chemical, redox, and electronic properties[2] as well as to their coordination behavior.

Metal−sulfur-based compounds find application in different technological fields such as catalysis,[3] photovoltaic materials,[4] magnetic resonance imaging and contrast agents,[5] semiconductor technology,[6] energy storage technology,[7] corrosion prevention, and tribology.[8] Most of these applications have been reviewed by Stiefel in a dedicated text,[9] while the

*To whom correspondence should be addressed. E-mail: silvia.gross@unipd.it (S.G.), luciano.pandolfo@unipd.it (L.P.).

(1) (a) Dance, I.; Fisher, K. In *Progress in Inorganic Chemistry*; Karlin, K. D., Ed.; Wiley-Interscience: New York, 1994. (b) Niu, J.; Zheng, H.; Hou, H.; Xin, X. *Coord. Chem. Rev.* **2004**, *248*, 169–183. (c) Fackler, J. P., Jr. *Prog. Inorg. Chem.* **1976**, *21*, 55–90. (d) Young, G. G. *J. Inorg. Biochem.* **2007**, *101*, 1562–1585. (e) *Handbook of Chalcogen Chemistry: New Perspectives in Sulfur, Selenium and Tellurium*; Devillanova, F., Ed.; Royal Society of Chemistry: London, England, 2006. (f) Dilworth, J. R.; Arnold, P.; Morales, D.; Wong, Y. L.; Zheng, Y. In *Modern Coordination Chemistry*; Leigh, G. J., Winterton, N., Eds.; Royal Society of Chemistry: Cambridge, U.K., 2002. (g) Schrauzer, G. N. *Adv. Chem. Ser.* **1972**, *110*, 73–91 (Sulfur Rec. Trends). (h) Clarke, C. S.; Haynes, D. A.; Rawson, J. M. *Annu. Rep. Prog. Chem., Sect. A: Inorg. Chem.* **2008**, *104*, 124–133.

(2) Kaim, W.; Hornung, F. M.; Schafer, R.; Fiedler, J.; Krejcik, M.; Zalis, S. High Technology. *Transition Metal Sulphides*; NATO ASI Series 3; Kluwer Academic: Varna, Bulgaria, 1998; *60*, pp 37−55.

(3) (a) Richards, R. L. *New J. Chem.* **1997**, *21*, 727–732. (b) Venkataramanan, N. S.; Kuppuraj, G.; Rajagopal, S. *Coord. Chem. Rev.* **2005**, *249*, 1249–1268.

(4) (a) McEvoy, A. J.; Grätzel, M. Photovoltaic Cells for Sustainable Energy. In *Sustainable Energy Technologies*; Hanjalic, K., Van De Krol, L. A., Eds.; Springer: The Netherlands, 2008; Chapter 5. (b) Goetzberger, A.; Hebling, C.; Schock, H. W. *Mater. Sci. Eng.* **2003**, *40*, 1–46.

(5) (a) Dithiolene Chemistry: Synthesis, Properties and Applications. In *Progress in Inorganic Chemistry*; Stiefel, E. I., Ed.; Wiley-Interscience: New York, 2004; Vol. *52*. (b) *Comprehensive Coordination Chemistry II* (*Technological Application of Coordination Chemistry*); McCleverty, J. A., Meyer, T. J., Eds.; Pergamon Press−Elsevier: The Netherlands, 2004; Vol. *9*.

(6) (a) Powalla, M.; Bonnet, D. *Adv. OptoElectron.* **2007**, 97545/1–97545/6. (b) Goetzberger, A.; Hebling, C.; Schock, H. W. *Mater. Sci. Eng.* **2003**, *R 40*, 1–46. (c) Mori, T. *J. Phys.: Condensed Matter* **2008**, *20*, 184010/1–184010/13.

(7) Tudron, F. B.; Akridge, J. R.; Puglisi, V. J. *Proc. Power Sources Conf.* **2004**, *41*, 341–344.

Published on Web 12/09/2010

relevance of sulfur in the field of life science, where many important electron-transfer proteins and enzymes involve the coordination of sulfur-containing ligands to different metals, has been extensively reported.[10]

A further intriguing aspect of metal−sulfur chemistry is the peculiar electronic structure characterizing M−S bonds, which has been the topic of a few reviews.[11] Particularly interesting is the formation of polynuclear complexes with metal−sulfur bonds because the electron polarizability, which give rises to M−S bridges and to the extended M−S-based networks, allows the formation of a delocalized electronic structure, which is, in turn, responsible for the outstanding properties of these polynuclear compounds.[1a,b]

A wide variety of sulfur ligands have been used to prepare polynuclear sulfur clusters[1a,b] with most of the metals.[1a,b,12−16] In this wide and manifold field, thiocarboxylic acids represent a versatile class of sulfur-based ligands and monothio- and dithiocarboxylates have been often reported as ligands in metal mono- and polynuclear complexes.[17−24]

In the past, we explored the synthesis of different early-transition-metal oxo clusters (with O−M−O moieties)[25] by the reaction of metal alkoxides with carboxylic acids, normally obtaining polynuclear structures. As demonstrated by these works, this early-transition-metal oxo cluster chemistry is mainly based on hydrolysis and condensation reactions involving the starting metal alkoxide precursor, which undergoes substitution reaction by the carboxylates. The cleaved alcohol further reacts with an excess of carboxylic acid in an esterification reaction.[26] The in situ formed water accounts for the hydrolysis/condensation reactions, leading to the formation of the O−M−O-based metal−oxo inorganic core, in a sui generis sol−gel reaction.

These polynuclear structures are typically obtained by reaction of the corresponding metal alkoxide with a carboxylic acid. They are characterized not only by different metals but also by manifold *nuclearity, structures and connectivity modes*, and *different functional groups*, which can enable, in a further synthetic step, their embedding into a matrix through reaction with suitable precursors.

Some review articles[25] have extensively described the chemistry of these polynuclear oxo clusters, whereas the mechanism leading to their formation and their ligand exchange dynamics has also been the topic of thorough studies.[25,26]

Cluster chemistry of zirconium is an established and mature field of research,[27] especially as far as zirconium halide clusters[28] are concerned. More recently, several authors[25,26,29] have focused on oxo and carboxylato clusters of zirconium also as precursors for the corresponding nanostructured oxide.[29b]

(8) *Sulfur, Its significance for Chemistry, for the Geo-, Bio- and Cosmosphere and Technology*; Mueller, A., Krebs, B., Eds.; Elsevier: Amsterdam, The Netherlands, 1984.

(9) *Transition Metal Sulfur Chemistry: Biological and Industrial Significance*; Stiefel, E. I., Matsumoto, K., Eds.; ACS Symposium Series 653; American Chemical Society: Washington, DC, 1996.

(10) (a) Groysman, S.; Holm, R. H. *Biochemistry* **2009**, *48*, 2310–2332. (b) Henkel, G.; Krebs, B. *Chem. Rev.* **2009**, *104*, 801–824. (c) Bertini, I.; Gray, H. B.; Stiefel, E. I.; Valentine, J. S. *Biological Inorganic Chemistry: Structure and Reactivity*; University Science Books: Sausalito, CA, 2007. (d) King, R. B.; Bitterwolf, T. E. *Coord. Chem. Rev.* **2000**, *206−207*, 563–579. (e) Mueller, A.; Diemann, E. *Trans. Met. Chem. Proc. Workshop* **1981**, 221–238. (f) Holm, R. H.; Kennepohl, P.; Solomon, E. I. *Chem. Rev.* **1996**, *96*, 2239–2314.

(11) (a) Joergensen, C. K. *Inorg. Chim. Acta* **1968**, *2*, 65–88. (b) Benedix, R.; Hennig, H. *Inorg. Chim. Acta* **1988**, *141*, 21. (c) Hadad, C. M.; Rablen, P. R.; Wilberg, K. B. *J. Org. Chem.* **1998**, *63*, 8668–8681. (d) Furlani, C.; Flamini, A.; Sgamellotti, A.; Bellitto, C. *J. Chem. Soc., Dalton Trans.* **1973**, *22*, 2404.

(12) Perruchas, S.; Flores, S.; Jousselme, B.; Lobkovsky, E.; Abruna, H.; DiSalvo, F. J. *Inorg. Chem.* **2007**, *46*, 8976–8987.

(13) (a) Melman, J. H.; Emge, T. J.; Brennan, J. G. *Inorg. Chem.* **1999**, *38*, 2117–2122. (b) Freedman, D.; Emge, T. J.; Brennan, J. G. *J. Am. Chem. Soc.* **1997**, *119*, 11112–11113. (c) Jin, G. B.; Choi, E. S.; Guertin, R. P.; Brooks, J. S.; Bray, T. H.; Booth, C. H.; Albrecht-Schmitt, T. E. *Chem. Mater.* **2007**, *19*, 567–574.

(14) (a) Hagen, K. S.; Christou, G.; Holm, H. *Inorg. Chem.* **1983**, *22*, 309–314. (b) Saak, W.; Henkel, G.; Pohl, S. *Angew. Chem.* **1984**, *96*, 153–154. (c) Saak, W.; Henkel, G.; Pohl, S. *Angew. Chem., Int. Ed. Engl.* **1984**, *23*, 150–151. (d) Betz, B.; Krebs, B.; Henkel, G. *Angew. Chem.* **1984**, *96*, 293–294. (e) Betz, B.; Krebs, B.; Henkel, G. *Angew. Chem., Int. Ed. Engl.* **1984**, *23*, 311–312. (f) Tremel, W.; Krebs, B.; Henkel, G. *Angew. Chem.* **1984**, *96*, 604–605. (g) Tremel, W.; Krebs, B.; Henkel, G. *Angew. Chem., Int. Ed. Engl.* **1984**, *23*, 634–635.

(15) (a) Mueller, A.; Henkel, G. *Chem. Commun.* **1996**, 1005–1006. (b) Tremel, W.; Krebs, B.; Henkel, G. *Inorg. Chim. Acta* **1983**, *80*, L31–L32. (c) Tremel, W.; Krebs, B.; Henkel, G. *J. Chem. Soc., Chem. Commun.* **1986**, 1527–1529. (d) Kriege, M.; Henkel, G. *Z. Naturforsch.* **1987**, *42b*, 1121–1128. (e) Kockerling, M.; Henkel, G. *Z. Kristallogr.* **2008**, *223*, 102–104.

(16) (a) Ali, B.; Dance, I. G.; Craig, D. C.; Scudder, M. L. *J. Chem. Soc., Dalton Trans.* **1998**, *10*, 1661–1667. (b) Albinati, A.; Casarin, M.; Maccato, C.; Pandolfo, L.; Vittadini, A. *Inorg. Chem.* **1999**, *38*, 1145–1152. (c) Albinati, A.; Casarin, M.; Eisentraeger, F.; Maccato, C.; Pandolfo, L.; Vittadini, A. *J. Organomet. Chem.* **2000**, *601*, 307–314. (d) Pandolfo, L.; Seraglia, R.; Venzo, A.; Gross, S.; Kickelbick, G. *Inorg. Chim. Acta* **2005**, *358*, 2739–2748.

(17) Chalcogenocarboxylic Acid Derivatives. In *Topics in Current Chemistry*; Kato, S., Vol. Ed.; Springer: The Netherlands, 2005; Vol. *251*.

(18) (a) Vittal, J. J.; Ng, M. T. *Acc. Chem. Res.* **2006**, *11*, 869. (b) Nyman, M. D.; Hampden-Smith, M. J.; Duesler, E. N. *Inorg. Chem.* **1997**, *36*, 2218–2224. (c) Santana, M. D.; Sáez-Ayala, M.; García, L.; Pérez, J.; García, G. *Eur. J. Inorg. Chem.* **2007**, 4628–4636. (d) Kinoshita, S.; Wakita, H.; Yamashita, M. *J. Chem. Soc., Dalton Trans.* **1989**, *12*, 2457–2459. (e) Macalindong, J. S.; Fronczek, F. R.; Schuerman, J. A.; Selbins, J.; Watkins, S. F. *Acta Crystallogr.* **2006**, *E62*, m889–m890. (f) Furlani, C.; Flamini, A.; Sgamellotti, A.; Bellitto, C. *J. Chem. Soc., Dalton Trans.* **1973**, 2404–2409.

(19) Mehrotra, R. C.; Srivastava, G.; Vasanta, E. N. *Inorg. Chim. Acta* **1980**, *47*, 125–130.

(20) Whitlow, S. *Acta Crystallogr.* **1975**, *B31*, 2531.

(21) Attanasio, D.; Bellitto, C.; Flamini, A. *Inorg. Chem.* **1980**, *19*, 3419–3424.

(22) Chaudhari, K. R.; Wadawale, A. P.; Ghoshal, S.; Chopade, S. M.; Sagoria, V. S.; Jain, V. K. *Inorg. Chim. Acta* **2009**, *362*, 1819–1824.

(23) Andras, M. T.; Duraj, S. A. *Inorg. Chem.* **1993**, *32*, 2874–2880.

(24) Duraj, S. A.; Andras, M. T.; Rihter, B. *Polyhedron* **1989**, *8*, 2763–2767.

(25) (a) Schubert, U. *J. Mater. Chem.* **2005**, *15*(35−36), 3701–3715. (b) Schubert, U. *J. Sol−Gel Sci. Technol.* **2004**, *31*(1/2/3), 19–24. (c) Schubert, U. *Macromol. Symp.* **2008**, *267*, 1–8 and references cited therein. (d) Albinati, A.; Faccini, F.; Gross, S.; Kickelbick, G.; Rizzato, S.; Tondello, E.; Venzo, A. *Inorg. Chem.* **2007**, *46*, 3459–3466. (e) Puchberger, M.; Kogler, F. R.; Jupa, M.; Gross, S.; Fric, H.; Kickelbick, G.; Schubert, U. *Eur. J. Inorg. Chem.* **2006**, *16*, 3283–3293. (f) Kickelbick, G.; Feth, M. P.; Bertagnolli, H.; Puchberger, M.; Holzinger, D.; Gross, S. *J. Chem. Soc., Dalton Trans.* **2002**, *20*, 3892–3898. (g) Walther, P.; Puchberger, M.; Kogler, F. R.; Schwarz, K.; Schubert, U. *Phys. Chem. Chem. Phys.* **2009**, *11*, 3640–3647.

(26) Bertagnolli, H.; Puchberger, M.; Holzinger, D.; Gross, S. *J. Chem. Soc., Dalton Trans.* **2002**, *20*, 3892–3898.

(27) (a) Draper, S. M.; Twamley, B. *Coord. Chem. Rev.* **1995**, *146*, 91–140. (b) Hughbanks, T. *J. Alloys Compd.* **1995**, *229*, 40–53. (c) Hughbanks, T. (McCleverty, J. A., Meyer, T. J., Eds.) *Compr. Coord. Chem. II* **2004**, *2*, 775−784. (d) Kumar, T. J. D.; Tarakeshwar, P.; Balakrishnan, N. *Phys. Rev. B: Condens. Matter Mater. Phys.* **2009**, *79*, 205415/1–205415/11. (e) Sun, Y.; Fournier, R.; Zhang, M. *Phys. Rev. A: At., Mol., Opt. Phys.* **2009**, *79*, 043202/1–043202/9.

(28) (a) Chen, L.; Cotton, F. A. *J. Cluster Sci.* **1998**, *9*, 63–91. (b) Koeckerling, M.; Qi, R.-Y.; Corbett, J. D. *Inorg. Chem.* **1996**, *35*, 1437–1443. (c) Corbett, J. D. *J. Alloys Compd.* **1995**, *229*, 10–23. (d) Runyan, C. E., Jr.; Hughbanks, T. *J. Am. Chem. Soc.* **1994**, *116*, 7909–7910. (e) Zhang, J.; Corbett, J. D. *Inorg. Chem.* **1995**, *34*, 1652–1656.

(29) (a) Zhong, W.; Alexeev, D.; Harvey, I.; Guo, M.; Hunter, D. J. B.; Zhu, H.; Campopiano, D. J.; Sadler, P. J. *Angew. Chem., Int. Ed.* **2004**, *43*, 5914–5918. (b) Otero, A.; Fernandez-Baeza, J.; Antinolo, A.; Tejeda, J.; Lara-Sanchez, A.; Sanchez-Barba, L.; Fernandez-Lopez, M.; Lopez-Solera, I. *Inorg. Chem.* **2004**, *43*, 1350–1358.

Table 1. Summary of Crystallographic Parameters for $\mathbf{Zr_3}$, $\mathbf{Zr_6}$, and $\mathbf{Zr_4}$

	$\mathbf{Zr_3}\cdot$2BuOH	$\mathbf{Zr_6}$	$\mathbf{Zr_4}$
formula	$C_{26}H_{44}O_2S_{18}Zr_3$	$C_{32}H_{52}O_{21}S_{13}Zr_6$	$C_{28}H_{48}O_{14}S_{10}Zr_4$
fw	1239.35	1736.84	1294.14
cryst size, mm	0.32 × 0.27 × 0.18	0.09 × 0.07 × 0.06	0.18 × 0.05 × 0.05
cryst syst	monoclinic	monoclinic	monoclinic
space group	$C2/c$	$P2_1/c$	$P2_1/n$
a, pm	1990.20(9)	1969.8(3)	1017.22(11)
b, pm	1644.69(8)	1473.29(19)	1346.39(14)
c, pm	1409.98(6)	2143.2(3)	1811.02(19)
β, deg	99.272(1)	95.130(2)	101.170(2)
$V \times 10^6$ [pm^3]	4554.9(4)	6194.9(14)	2433.3(4)
Z	4	4	2
ρ_{calcd}, g cm^{-3}	1.807	1.862	1.766
μ(Mo Kα), mm^{-1}	1.526	1.473	1.316
θ_{max}, deg	28.33	28.31	27.50
reflns measd	25 482	42 823	15 851
unique reflns	25 546	15 359	5563
rflns $I > 2\sigma(I)$	21 434	10 072	4414
param	238	784	258
restraints	67	422	0
R1 [$I > 2\sigma(I)$]	0.0328	0.0477	0.0303
wR2 [$I > 2\sigma(I)$]	0.0845	0.1178	0.0665
GOF for I^2	1.025	1.019	1.007
min/max, e Å^{-3}	0.656/−0.654	2.447/−1.305	0.774/−0.679

Table 2. Summary of Bond Lengths [pm] for $\mathbf{Zr_3}$

	$\mathbf{Zr_3}$
core	Zr1−S11 265.16(4), Zr1−S12′ 265.69(4), Zr1−S13 265.14(4), Zr1−S13′ 264.90(4), Zr2−S11 264.36(3), Zr2−S12 266.24(4)
μ_3-SSSCCH$_3$	S11−C11 182.96(14), S12−C11 183.44(14), S13−C11 182.87(15)
μ_1-SSCCH$_3$	Zr1−S21 268.97(4), Zr1−S22 262.96(4), Zr1−S31 264.17(4), Zr1−S32 268.97(4), Zr2−S41 270.37(4), Zr2−S42 262.59(4)

In the present work, we used monothioacetic acid to coordinate zirconium (added as butoxide), generating polynuclear clusters, with a behavior in some way related to what was observed with the homologue carboxylic acids that we employed in the past.

2. Experimental Section

2.1. Material and Methods. All reactions and manipulations were carried out under an argon atmosphere using standard Schlenk or septum/cannula techniques. Zr(O^{n}Bu)$_4$ (80%) in *n*-butanol (purchased by ABCR GmbH, Karlsruhe, Germany) and anhydrous *n*-butanol (99+%; purchased by Aldrich, Milan, Italy) were stored under an argon atmosphere and not further purified. Monothioacetic acid (TAA; 96%; purchased by Aldrich, Milan, Italy) was used as received. The hydrogen sulfide flask was supplied by Aldrich, Milan, Italy.

2.2. Raman Analysis. Raman analyses were carried out with a Thermo Scientific Nicolet DXR Raman microscope. The details on the equipment and analyses are reported in the Supporting Information. Two samples were characterized through Raman spectroscopy: crystalline compound $Zr_4(\mu_3\text{-}O)_2(\mu\text{-}\eta^1\text{-}SOCCH_3)_2(SOCCH_3)_8(O^nBu)_2$ ($\mathbf{Zr_4}$), synthesized with a molar ratio Zr/TAA of 1:8, and monothioacetic acid as the reference. They were put in capillary tubes under an argon atmosphere in order to avoid air contact. Raman spectrum of liquid monothioacetic acid: 2919 (s, sh, ν_{CH}), 2574 (s, sh, ν_{SH}), 1706 (m, $\nu_{C=O}$ in C(O)SH), 1427 (w), 1134 (w), 999 (w), 839 (w), 629 (s, sh), 450 (s, sh), 329 (w), 145 (w).

2.3. NMR Experimental Part. The ^{1}H and ^{13}C NMR spectra were obtained at 298 K as C_6D_6 solutions with a Bruker DMX-400 Avance spectrometer operating at ν_0 400.13 and 100.61 MHz, respectively. Details on the experiments (COSY, TOCSY, NOESY, HMQC, and BIRD)[30a,b,c] performed and chemical shift assignments are reported in the Supporting Information.

2.4. X-ray Crystallography Experimental Part. Crystals of $\mathbf{Zr_3}$, $\mathbf{Zr_4}$, and $\mathbf{Zr_6}$ suitable for single-crystal X-ray diffraction were taken directly from reaction mixtures, selected in perfluoropolyether oil, mounted on a Bruker AXS Kappa diffractometer with an APEX II CCD area detector, and measured in a nitrogen stream at 100 K. Graphite-monochromated Mo Kα radiation (λ = 71.073 pm) was used for all measurements. Further details on the experiments are reported in the Supporting Information.

The structures were solved with direct methods and then refined by the full-matrix least-squares method based on F^2 using the program package *SHELXTL* (Bruker AXS). All non-H atoms were refined anisotropically. H atoms on C atoms were inserted and refined riding on their parent atoms.

Important parameters for all structures are summarized in Table 1. Selected bond lengths are summarized in Table 2 for $\mathbf{Zr_3}$ and in Table 3 for $\mathbf{Zr_6}$ and $\mathbf{Zr_4}$.

$\mathbf{Zr_3}$ [$Zr_3(\mu_3\text{-}S_3CCH_3)_2(S_2CCH_3)_6]\cdot 2^n$BuOH: disordered ^{n}BuOH was found and refined in channels between the cluster molecules; a distinction between the C and OH end was not possible. Therefore, all atoms were refined as C atoms.

$\mathbf{Zr_6}$ [$Zr_6(\mu_3\text{-}O)_5(\mu\text{-}SOCCH_3)_2(\mu\text{-}O_2CCH_3)(SOCCH_3)_{11}$-(^{n}BuOH)]: two of the unbridging $SOCCH_3$ groups were refined disordered over two positions with occupancies 0.89:0.11 and 0.74:0.26. O131 of the μ-O_2CCH_3 ligand has an elongated thermal ellipsoid. This could be improved when additionally an S atom with occupancy 0.06 (and O131 with occupancy 0.94) was refined on the position of the residual electron density maximum, which was situated 69 pm from O131 and 257 pm from Zr5. However, the anisotropic parameters of this S atom were nonpositive definite. Therefore, μ-O_2CCH_3 was substituted by μ-monothioacetate by around 6%, but it was not implemented in the structure refinement. The ^{n}BuOH group was refined disordered over two positions (0.57:0.43), although there are probably at least three different positions. The highest

(30) (a) Bax, A.; Subramanian, S. *J. Magn. Reson.* **1986**, *67*, 565. (b) Otting, G.; Wüthrich, K. *J. Magn. Reson.* **1988**, *76*, 569. (c) Bax, A.; Summers, M. F. *J. Am. Chem. Soc.* **1986**, *108*, 209. (d) Drobny, G.; Pines, A.; Sinton, S.; Weitekamp, D.; Wemmer, D. *Faraday Symp. Chem. Soc.* **1979**, *B33*, 4912.

Table 3. Summary of Bond Lengths [pm] for Zr_6 and Zr_4

	Zr_6	Zr_4
Core	Zr1−O1 220.5(4), Zr1−O2 222.5(4), Zr1−O3 206.9(4), Zr1−O4 213.8(4), Zr1−O5 218.7(4), Zr2−O1 209.8(4), Zr2−O5 204.5(4), Zr3−O1 197.7(4), Zr3−O2 202.6(4), Zr4−O3 205.1(4), Zr4−O2 208.5(4), Zr5−O3 201.9(4), Zr5−O4 209.3(4)	Zr1−O1 210.62(18), Zr2−O1 213.1(2), Zr2−O1′ 203.53(19)
μ_1-$SOCCH_3$	Zr4−O08 229.3(4), Zr4−O091 224.1(9), Zr4−O093 222.4(16), Zr4−O10 230.1(4), Zr4−S08 265.87(16), Zr4−S091 270.9(3), Zr4−S093 267.5(9), Zr4−S10 276.03(17), Zr2−O04 224.4(4), Zr2−O031 230.7(8), Zr3−O05 224.1(4), Zr3−O06 223.7(4), Zr5−O11 226.5(4), Zr5−O12 226.8(5), Zr6−O14 221.7(5), Zr6−O15 223.9(5), Zr2−S04 271.61(17), Zr2−S031 270.8(2), Zr3−S05 269.20(16), Zr3−S06 267.63(17), Zr5−S11 269.95(17), Zr5−S12 272.85(18), Zr6−S14 271.76(18), Zr6−S15 270.24(18), Zr5−O10 271.5(4)	Zr1−O2 224.3(2), Zr1−O3 224.7(2), Zr2−O5 224.5(2), Zr2−O6 224.6(2), Zr1−S2 270.11(9), Zr1−S3 268.56(8), Zr2−S5 266.76(8), Zr2−S6 267.35(8)
μ_2-$SOCCH_3$	Zr1−O01 209.2(4), Zr1−O02 208.0(4), Zr2−S01 274.66(17), Zr2−S02 281.63(16)	Zr2−O4 234.13(19), Zr2−S4 276.40(8), Zr1−O4 228.6(2)
μ_1-(H)O^{n}Bu	Zr3−O071 222.0(8), Zr3−O075 217.9(10)	Zr1−O11 187.2(2)
μ_2-$OOCCH_3$	Zr5−O131 218.9(5), Zr6−O132 217.4(4)	

residual electron density peak (2.45) was found at 216 pm from C074 of the ^{n}BuOH. This could be explained by partial occupation by a small molecule, e.g., monothioacetic acid.

Zr_4 [$Zr_4(\mu_3\text{-}O)_2(\mu\text{-}SOCCH_3)_2(SOCCH_3)_8(O^nBu)_2$]: The ^{n}BuO ligand was refined with very small anisotropic parameters, even for the terminal C atoms. The Zr−O distance was 187.2(2) pm, which is in good agreement with values reported in the literature for Zr−O^{n}Bu coordination (see the discussion for **Zr_6**).

CCDC 779090 (for **Zr_3**), 779091 (for **Zr_4**), and 779092 (for **Zr_6**) contain the supplementary crystallographic data for this paper. These data can be obtained free of charge from the Cambridge Crystallographic Data Centre via www.ccdc.cam.ac.uk/data_request/cif.

2.5. Extended X-ray Absorption Fine Structure (EXAFS) Measurements. Sample Preparation. The solution for EXAFS analysis was prepared with the same procedure as that employed for the synthesis of the clusters, using an alkoxide/TAA molar ratio of 1:6.

EXAFS Measurements and Data Evaluation. The EXAFS measurements were performed at Beamline C1 of the Hamburger Synchrotronstrahlungslabor (HASYLAB) at DESY (Hamburg, Germany). They were performed at the Zr K-edge (17998.0 eV) using a Si(311) double crystal monochromator. A detailed description of the experiments and the procedure adopted for data evaluation[31] and processing are reported in the Supporting Information.

3. Syntheses

3.1. Synthesis of $Zr_4(\mu_3\text{-}O)_2(\mu_2\text{-}\eta^1\text{-}SOCCH_3)_2(SOCCH_3)_8(O^nBu)_2$ (Zr_4). To an 80% solution in ^{n}BuOH of $Zr(O^nBu)_4$ (2.67 g, 5.6 mmol) monothioacetic acid (3.2 mL, 44.6 mmol) was added at 298 K (molar ratio Zr/TAA = 1/8). After the addition of TAA, evolution of H_2S was observed, which was removed from the Schlenk-tube through repeated venting. The reaction mixture was then allowed to stand at room temperature for 7 days, resulting in the separation of yellow, rectangular crystals. The crystals are soluble in acetone, benzene, and dimethyl sulfoxide.

NMR Analysis. The NMR spectra of the oxothio cluster **Zr_4** were recorded as C_6D_6 solutions because of the instability of these species in deuterated acetone and dimethyl sulfoxide. Nevertheless, besides core-bonded *n*-butoxy and monothioacetate peaks, the spectra showed as most relevant signals those pertaining to *n*-butyl acetate, likely due to the presence of adventitious water. The spectra showed as the most relevant signals those due to *n*-butyl acetate, reported below.

n-Butyl acetate. ^{1}H NMR: δ 0.854 (m, 3H), 1.285 (m, 2H), 1.494 (m, 2H), 1.842 (s, 3H), 4.045 (m, 2H). ^{13}C NMR: δ 14.36, 20.01, 21.12 (acetyl CH_3), 31.66, 64.62, and 170.61 (CO).

Core-bonded *n*-butoxy groups (all resonances broaden). ^{1}H NMR: δ 0.97, ca. 1.2, ca. 1.6, ca. 4.2. ^{13}C NMR: δ 14.9, ca. 21, 36.7, ca. 73.

Monothioacetate groups (all resonances broaden). ^{1}H NMR: δ 2.41, 2.43, 2.51, 2.55, 2.62, 2.67, 2.69. ^{13}C NMR: δ 36.6 and 45.9 (CH_3), 220.0, 222.2, 226.4, 230.2, 231.4, 232.8, 233.0, 234.0, 261.3, 265.2, 267.0, and 268.7 (thiocarbonyl).

Raman Analysis. The Raman spectrum of the oxothio cluster **Zr_4** (Figure 4) was recorded on the crystals, whereas that of the monothioacetic acid was recorded directly on the liquid specimen. The obtained spectra were analyzed by using literature data.[33]

Raman data of **Zr_4**: 2914 (s, sh, ν_{CH}), 1464 (w), 1352 (w), 1178 (m), 707 (s, sh), 574 (m, br), 531 (w), 380 (w), 246 (m, sh), 206 (m).

3.2. Synthesis of $Zr_6(\mu_3\text{-}O)_5(\mu\text{-}SOCCH_3)_2(\mu\text{-}O_2CCH_3)(SOCCH_3)_{11}(^nBuOH)$, ($Zr_6$). To an 80% solution in ^{n}BuOH of $Zr(O^nBu)_4$ (1.60 g, 3.3 mmol) monothioacetic acid (1.9 mL, 26.7 mmol) was added at 288 K (molar ratio Zr/TAA = 1/8). After the addition of TAA, evolution of H_2S was observed, which was removed from the Schlenk-tube through mild venting.

The reaction mixture was then allowed to stand 30 days at 278 K, resulting in the separation of yellow, rectangular-shaped crystals.

3.3. Synthesis of $Zr_3(\mu_3\text{-}S_3CCH_3)_2(S_2CCH_3)_6$ (Zr_3). From the same reaction batch of **Zr_6**, maintained at 278 K, after 60 days red crystals separated from the reaction mixture. The same crystal formed exclusively when H_2S was added (see below) to the reaction system of the synthesis of **Zr_6**.

(31) (a) Binsted, N.; Hasnain, S. S. *J. Synchrotron Radiat.* **1996**, *3*, 185. (b) Binstad, N. In *EXCUR98 Manual*; Mosselmans, F., Ed.; CCLRC Daresbury Laboratory: Warrington, Cheshire, U.K.,1998.

(32) Zabinsky, S. I.; Rehr, J. J.; Ankudinov, A.; Albers, R. C.; Eller, M. J. *Phys. Rev. B* **1995**, *52*, 2995.

(33) (a) Nakamoto, K. *Infrared Spectra of Inorganic and Coordination Compounds*; John Wiley and Sons: New York, 1997. (b) Socrates, G. *Infrared and Raman Characteristic Group Frequencies*; John Wiley and Sons Ltd.: Chichester, U.K., 2001. (c) Roubi, L.; Carlone, C. *Phys. Rev. B* **1988**, *37*, 6807. (d) Ali, A. A. M.; Zaki, M. I. *Thermochim. Acta* **2002**, *387*, 29–38. (e) Butler, I. S.; Harvey, P. D.; McCall, J. M.; Shaver, A. *J. Raman Spectrosc.* **1986**, *17*, 221–228. (f) Clark, R. J. H.; Walton, J. R. *Inorg. Chim. Acta* **1987**, *129*, 163–171.

Table 4. Results of the Reactions and Structures Obtained (M = Metal; L = Monothioacetic Acid)

M:L	T (K), conditions	product(s)	structure	Dt_{pr} (days)
1:8	288, Ar	Zr_6 (yellow)	$Zr_6O_5(SOCCH_3)_{13}(O_2CCH_3)(C_4H_9OH)$	30
		Zr_3 (red)	$Zr_3(S_3CCH_3)_2(S_2CCH_3)_6$	60
1:4	288, Ar	Zr_3 (red)	$Zr_3(S_3CCH_3)_2(S_2CCH_3)_6$	60
1:8	298, Ar	Zr_4 (yellow)	$Zr_4O_2(SOCCH_3)_{10}(C_4H_9O)_2$	0−10
1:5	273, Ar; 263, Ar	Zr_4 (yellow)	$Zr_4O_2(SOCCH_3)_{10}(C_4H_9O)_2$	10
1:5	excess of H_2S	small, red crystals	$Zr_3(S_3CCH_3)_2(S_2CCH_3)_6$	30

It is worth noting that, in all of the reactions of $Zr(O^nBu)_4$ with TAA, the development of H_2S was observed, which was removed from the reaction batches by venting.

3.4. Synthesis of Zr_3 in the Presence of H_2S. To an 80% solution in ^{n}BuOH of $Zr(O^nBu)_4$ (2.07 g, 4.3 mmol), prepared at 263 K was added monothioacetic acid (1.8 mL, 26.0 mmol) at 263 K (molar ratio Zr/TAA = 1/6). Then H_2S was added in excess, maintaining the system in anhydrous conditions. After the addition of TAA and H_2S, further evolution of H_2S was not observed as long as the temperature system was maintained at lower than 268 K. At a temperature of 268 K, considerable evolution of gas (H_2S) was observed, which was removed from the Schlenk-tube through venting. After 30 min, the reaction mixture was allowed to stand at room temperature for 3 h and then at 278 K for 30 days, resulting in the separation of dark-red crystals, identical with those of **Zr_3**.

4. Results and Discussion

As demonstrated by previous works, this early-transition-metal oxo cluster chemistry is mainly based on hydrolysis and condensation reactions involving the starting metal alkoxides precursor, which undergoes substitution reaction by the carboxylates. The alcohol further reacts with an excess of carboxylic acid in an esterification reaction,[28] and the in situ formed water accounts for the hydrolysis/condensation reactions, leading to the formation of the O−M−O-based metal−oxo inorganic core, in a sui generis sol−gel reaction.

In this study, we aimed to explore the possibility of extending the well-known *oxo* cluster chemistry[25−28,34,35] to the formation of analogous *thiooxo* and *dithio* cluster structures.

The research in this framework is driven by the impact on the basic structural and inorganic chemistry of metal−sulfur compounds as well as, as was already outlined, by possible applications in a number of fields based on compounds characterized by different electronic structures, with respect to their oxygen-based homologues. In this framework, the formation of heteroleptic complexes, with S,O or S,S ligands *chelating* the same metal ion, turns out to be particularly interesting because the S−M−O and S−M−S fragments are expected to be characterized by electronic properties significantly different from those of the O−M−O one.

Concerning zirconium, Coucouvanis et al.[36,37] explored the synthesis and structural characterization of different Zr−S polynuclear clusters, both trinuclear and hexanuclear, whereas other chalcogenido complexes of zirconium have been reported by Howard et al.[38] and Kekia and Rheingold.[39]

However, to the best of our knowledge, both monothioacetic and dithioacetic acid have not yet been employed for the synthesis of thiozirconium polynuclear clusters. Therefore, we started our studies by reacting monothioacetic acid with zirconium *n*-butoxide at room temperature and, in the absence of a solvent, by slightly changing the reaction conditions (molar ratios, reaction temperature, etc.) in different experiments. In Table 4, the experimental conditions for the obtainment of the different clusters are summarized, together with the other reaction conditions, leading to the formation of crystals that were, however, not structurally resolved.

As described above, the reactions were performed by varying the Zr/TAA molar ratio and by adding ex situ H_2S to the reaction batch (see Table 4). Moreover, further experiments were carried out to investigate how modification of the other experimental conditions (temperature, solvent, solvent removal, etc.) affected the evolution of the system. In particular, we first changed the temperature at which the reaction occurred in the range from −15 to +27 °C. The effect of this variation was, upon a temperature decrease, mainly to slow down the formation of the solid precipitate. At low temperature (−15 °C), the observed growth of the crystals was extremely slow, whereas at room temperature (27 °C), sudden precipitation of a microcrystalline solid was instead observed. Concerning the addition of a solvent, one attempt was carried out by using anhydrous THF [molar ratios: $Zr(OBu)_4$/TAA/THF = 1/4/1 at 20 °C]. In this case, the solution remained clear and stable for 6 months.

The reactions were accordingly carried out without the addition of solvent(s) because the presence of a liquid phase was already provided by the nature of the precursors, both liquid [TAA and 80% $Zr(OBu)_4$ in butanol]. As far as the removal of excess butanol and the liquid phase is concerned, this led invariably to degradation of the formed crystals.

About the kinetics of crystal formation, some general considerations can be made. (i) The formation of different crystals occurs always in the same sequence: first, the yellow rectangular-shaped crystals (**Zr_6**) and, after a time span of about 60 days, red crystals (**Zr_3**). (ii) The formation of **Zr_4** seems to be favored by lower temperatures; the formation of the **Zr_3** crystals containing *only* S−M−S bonds does require longer time. (iii) The ex situ addition of H_2S promotes the selective formation of red crystals of **Zr_3**.

From the latter two points, it can be concluded that the selective formation of **Zr_3** is triggered by the presence of S^{2-} either added ex situ as H_2S or formed in situ upon hydrolysis of monothioacetic acid (see Scheme 2SM in the Supporting Information). This latter reaction requires longer times, thus explaining the slower formation of the **Zr_3** crystals.

(34) Kogler, F. R.; Jupa, M.; Puchberger, M.; Schubert, U. *J. Mater. Chem.* **2004**, *14*, 3133–3138.
(35) Moraru, B.; Gross, S.; Kickelbick, G.; Trimmel, G.; Schubert, U. *Monatsh. Chem.* **2001**, *132*, 993–999.
(36) Coucouvanis, D.; Lester, R. K.; Kanatzidis, M. G.; Kessisoglou, D. *J. Am. Chem. Soc.* **1985**, *107*, 8279–8280.
(37) Coucouvanis, D.; Hadjikyriacou, A.; Kanatzidis, M. G. *J. Chem. Soc., Chem. Commun.* **1985**, 1224–1225.
(38) Howard, W. A.; Trnka, T. M.; Parkin, G. *Inorg. Chem.* **1995**, *34*, 5900–5909.
(39) Kekia, O. M.; Rheingold, A. L. *Organometallics* **1997**, *16*, 5142–5147.

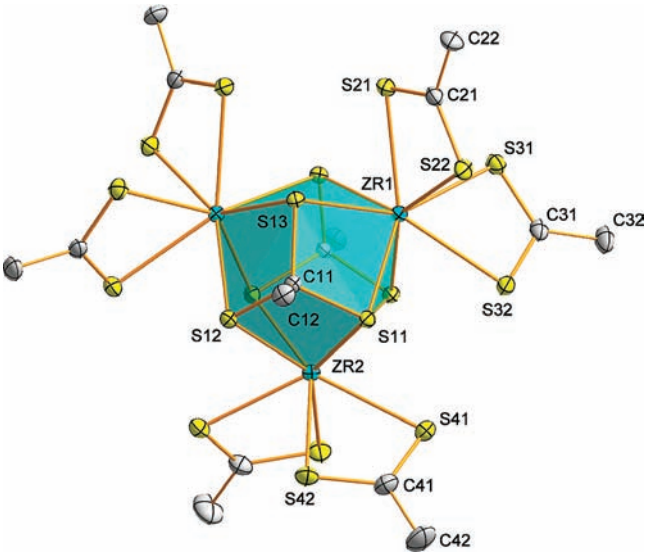

Figure 1. Crystal structure of $\mathbf{Zr_3}$. H atoms were omitted for clarity.

It should be pointed out that all of the obtained crystals are highly sensitive to air and humidity and rapidly hydrolyze upon exposure to air. For this reason, we restricted our analyses to only the samples reported in Table 4. In all of the syntheses, the fast development of H_2S, which had to be removed from the Schlenk-tube by outgassing, was observed upon the addition of monothioacetic acid to zirconium butoxide (see section 4.5). As discussed in section 4.5, the presence of hydrogen sulfide promotes the formation of the trinuclear cluster.

4.1. Description of the Crystal Structures. Three new polynuclear complexes were characterized by single-crystal X-ray diffraction. In the following, the three X-ray structures are discussed.

Zr_3. The crystallographic symmetry of the cluster is C_2, with the 2-fold axis passing through Zr2 (Figure 1). However, the molecular symmetry of the cluster is D_3, with a 3-fold axis through the C−Me groups of the S_3CCH_3 ligands. Three Zr atoms form a nearly equilateral triangle and are capped by two μ_3-S_3CCH_3 ligands. The Zr−Zr, Zr−S, and S−C distances are in the range 385.97(3)−387.04(3), 264.36(3)−266.24(4), and 182.96(14)−183.44(14), respectively. Each Zr atom is coordinated by four S atoms from the two capping μ_3-S_3CCH_3 ligands and four S atoms from the two chelating S_2CCH_3 ligands, which leads to the coordination number 8 for all Zr atoms. The Zr−S distances for the S_2CCH_3 ligands are in the range 262.96(4)−270.37(4) pm. The presence of a μ_3-S_3CCH_3 ligand with similar coordination behavior was previously found in a nickel complex [$Ni_3(\mu_3$-$S_3CCH_3)(S_2CCH_3)_3$],[40] although the S−C distances for the μ_3-S_3CCH_3 ligand are in a broader range there (176−199 pm). The origin of μ_3-S_3CCH_3 and S_2CCH_3 ligands in $\mathbf{Zr_3}$ will be discussed in section 4.5.

The same cluster crystallizes also in another crystal form with one ^{n}BuOH per cluster. It has the same space group but different cell parameters [a = 2007.6(2) pm, b = 1675.62(19) pm, c = 1552.0(3) pm, β = 125.247(1)°, V = 4263.9(11) pm^3].

(40) Bonamico, M.; Dessy, G.; Fares, V.; Scaramuzza, L. *J. Chem. Soc., Dalton Trans.* **1975**, *23*, 2594–2597.

Zr_6. The core of this oxo cluster (Figure 2) is formed by a planar star-shaped pentagon with one Zr atom in the center, five Zr atoms in the tips, and five O atoms, each bridging three Zr atoms, with one of them being the central Zr atom. The maximum deviations of Zr and O atoms in the star from the plane calculated through all Zr atoms are only 7.24(4) and 6.5(4) pm, respectively, and the sum of the bond angles around the μ_3-O atoms is close to 360°. The $Zr_{center}-Zr_{tip}$, $Zr_{center}-\mu_3$-O, and $Zr_{tip}-\mu_3$-O distances are in the ranges 330.13(8)−341.15(9), 206.9(4)−222.5(4), and 197.7(4)−209.8(4) pm, respectively.

In this cluster, the variable coordination behavior of the Zr atoms is noteworthy; each Zr atom has a different coordination environment (Table 5). The connection between the individual Zr atoms is mediated mainly through oxo bridges; only Zr1 and Zr2 are connected also by two μ_2-$SOCCH_3$ ligands on both sides of the star plane [distance Zr1−O = 208.0(4) and 209.2(4) pm; Zr2−S = 274.66(17) and 281.63(16) pm], and Zr5 and Zr6 are connected by a μ-O_2CCH_3 (to ∼5% μ-$SOCCH_3$; for details, see the Experimental Part) ligand in the star plane [distance Zr−O = 217.4(4) and 218.9(5) pm].

There is also a weak interaction between the O atom of a $SOCCH_3$ chelating ligand on Zr4 and the adjacent Zr5 [distance Zr5−O10 = 271.5(4) pm]. The distance is much longer than the similar one in $\mathbf{Zr_4}$, maybe also because of the higher coordination number of Zr5 ($\mathbf{Zr_6}$) than that of Zr1 ($\mathbf{Zr_4}$). This ligand lies also in the Zr plane [deviations are 26.1(5) pm for O10 and 9.65(18) pm for S10]. All other monothioacetate ligands are chelating.

The $Zr(SOCCH_3)_3$ and $Zr(SOCCH_3)_2$ coordination modes are present in the cluster. The $Zr_{tip}-O$ and $Zr_{tip}-S$ distances are in ranges of 221.7(5)−230.7(8) and 265.87(16)−276.03(17) pm, respectively. This leads to zirconium coordination numbers of 7−8. M(thiocarboxylate)$_x$ (x = 2, 3) coordination has not often been reported for transition-metal complexes.

The presence of a ^{n}BuOH ligand (rather than ^{n}BuO) was confirmed by the rather long distance Zr3−O71/O75 = 222.0(8)/217.9(10) pm, although the H atom was not found in the residual electron density (for details, see the Experimental Part). For comparison, typical Zr−O distances of the Zr−OR groups are in the range 195−200 pm, while a Zr−O distance of 228.6(5) pm was found for the coordinated n-butanol molecule in $Zr_6O_4(OH)_4$(methacrylate)$_8$(isobutyrate)$_4$(BuOH).[32]

Zr_4. This cluster is built from two $Zr_2(SOCCH_3)_5(O^nBu)$ units connected by two oxo bridges and related by an inversion center (Figure 3). Its crystallographic symmetry is C_i, but the molecular symmetry is almost C_{2h} if we do not take into account the ^{n}BuO ligands. Its core is formed by four Zr atoms, which lie exactly in a plane, and two O atoms, which connect three Zr atoms each and are located 0.23(19) pm off the Zr plane. Furthermore, Zr1 and Zr2 are connected by the O atom of a bridging−chelating $\mu-\eta^1$-$SOCCH_3$ ligand, which is also approximately located in the Zr_4 plane [4.4(2) pm off the Zr plane for O4 and 1.19(10) pm for S4]. The Zr−O distances in the core lie in the range 203.5−213.1 pm. In the $\mu-\eta^1$-$SOCCH_3$ ligand, the Zr−O distance to the adjacent Zr1 is even shorter than that to Zr2 [distance Zr2−O4 = 234.13(19) pm, Zr1−O4 = 228.6(2) pm, and Zr2−S4 = 276.40(8) pm]. Besides this, all Zr atoms are coordinated

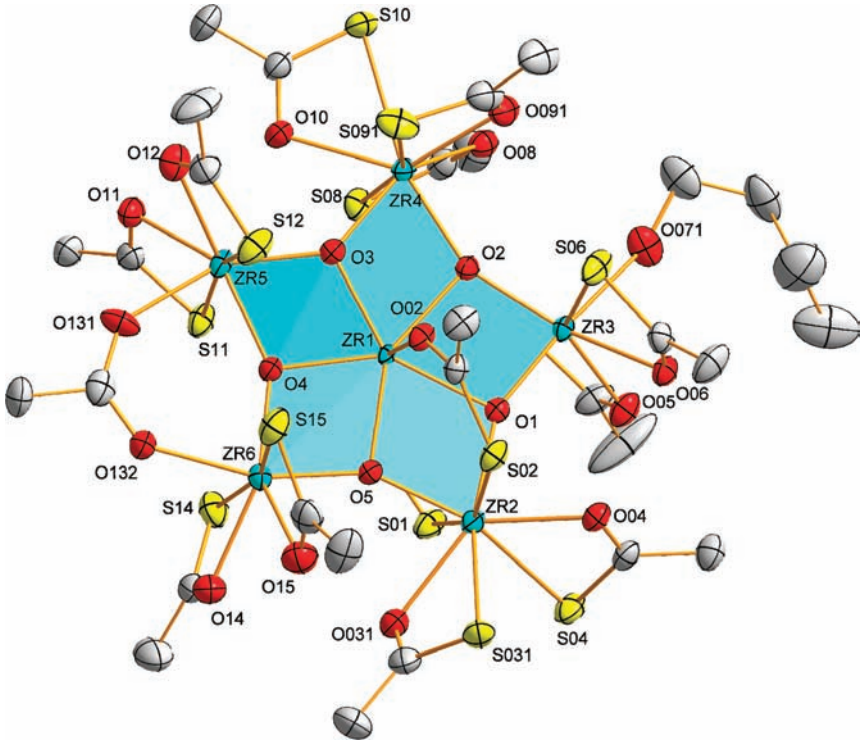

Figure 2. Crystal structure of $\mathbf{Zr_6}$. H atoms were omitted for clarity.

Table 5. Summary of the Coordination Modes of Zr Atoms in $\mathbf{Zr_6}$

Zr atom	coord. no.	ligands
Zr1	7	5 × O, 2 × O(μ_2-SOCCH$_3$)
Zr2	8	2 × O, 2 × S(μ_2-SOCCH$_3$), 2 × S,O(SOCCH$_3$)
Zr3	7	2 × O, 2 × S,O(SOCCH$_3$), 1 × O(HO*n*Bu)
Zr4	8	2 × O, 3 × S,O(SOCCH$_3$)
Zr5	7(8)	2 × O, 2 × S,O(SOCCH$_3$), 1 × O(μ_2-O$_2$CCH$_3$), 1 × O(SOCCH$_3$)
Zr6	7	2 × O, 2 × S,O(SOCCH$_3$), 1 × O(μ_2-O$_2$CCH$_3$)

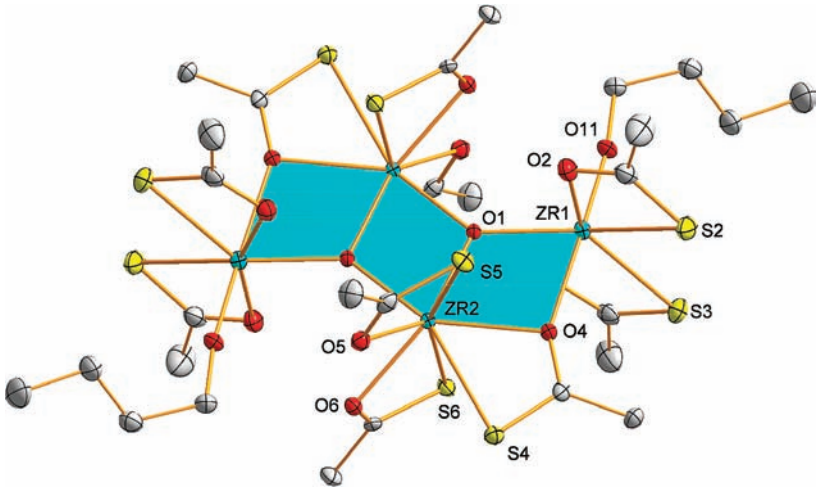

Figure 3. Crystal structure of $\mathbf{Zr_4}$. H atoms were omitted for clarity.

by two chelating SOCCH$_3$ ligands, Zr1 additionally by a terminal O^{n}Bu ligand. This results in coordination numbers of 7 and 8 for Zr1 and Zr2, respectively. The Zr−O and Zr−S distances for unbridging SOCCH$_3$ ligands are in the ranges 224.3(2)−224.7(2) and 266.76(8)−270.11(9) pm, respectively. The distance Zr1−O11 = 187.2(2) pm shows that the ^{n}BuO ligand is deprotonated because the distance Zr1−O11 is much shorter than the equivalent bond for the ^{n}BuOH ligand in $\mathbf{Zr_6}$.

To the best of our knowledge, such a μ−η^1 coordination of thiocarboxylate ligands, where O is bridging and S coordinates to the parent metal, has, to our knowledge, not yet been reported for transition-metal complexes.

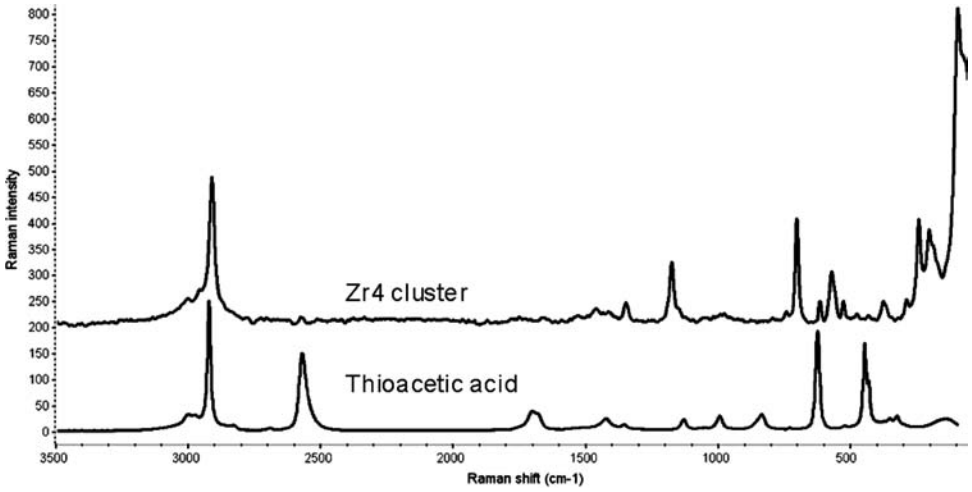

Figure 4. Raman spectra of monothioacetic acid (a) and $\mathbf{Zr_4}$ (b).

4.2. Raman Analysis of $\mathbf{Zr_4}$. Monothioacetic acid and the crystalline $\mathbf{Zr_4}$ cluster were additionally analyzed by Raman spectroscopy performed under an argon atmosphere. The two spectra are superimposed in Figure 4.

The assignment of the peaks was carried out on the basis of (i) the very few references present in the literature on Raman spectra of compounds containing Zr−S bonds,[31] (ii) a comparison with monothioacetic acid, and (iii) consideration of the cluster structure.

Both the spectra of $\mathbf{Zr_4}$ and TAA present a sharp and intense band at about 2914−2919 cm^{-1}, ascribed to C−H stretching.[31a,b]

On the contrary, the sharp peak corresponding to the S−H stretching at 2574 cm^{-1} in the spectrum of TAA is not present in the spectrum of the cluster $\mathbf{Zr_4}$, in agreement with the crystal structure, which evidences deprotonation of monothioacetic acid upon coordination to the Zr atoms.[31a,b] Accordingly, in the $\mathbf{Zr_4}$ spectrum also C═O stretching of the undissociated acid at 1706 cm^{-1} disappears upon coordination. Instead, a sharp band at 1179 cm^{-1} is present, which can be ascribed to C−S stretching in the monothioacetate species.[31f] The band at 706 cm^{-1} would correspond, accordingly, to C−S deformation.

The most interesting zone is that in the range 380−200 cm^{-1}, where the metal−oxygen and metal−sulfur stretchings are expected. By comparison with the spectrum of the reference acid and with the literature data,[31] the band at 246 cm^{-1} in the cluster spectrum is ascribed to the Zr−S E_g phonon frequency, whereas that at 291 cm^{-1} could be assigned to Zr−O. The assignment of this latter band is, however, challenging because at 300 cm^{-1} also the symmetric Zr−S stretching would be expected;[31] in fact, both bonds (Zr−S and Zr−O) are present in the tetranuclear cluster structure (see Figure 3).

4.3. NMR Spectra of $\mathbf{Zr_4}$ Solutions in $\mathbf{C_6D_6}$. The solution behavior of the cluster $\mathbf{Zr_4}$ was investigated by ^1H and ^{13}C NMR mesurements. Most of the resonances are attributed to *n*-butyl acetate (see the Experimental Section). An additional set of four, less intense, broad resonances (see the Experimental Section) is attributed to *n*-butoxy units reasonably bonded to the metal core. Moreover, another set of less intense and broader ^1H NMR resonances in the ranges 2.34−2.44 and 2.63−2.67 ppm correlate in the $^1H-^{13}C$ HMQC heteronuclear one-bond correlation map with broad ^{13}C NMR resonances at 36.6 and 45.9 ppm, respectively, and in the $^1H-^{13}C$ HMBC multiple-bond heteronuclear correlation spectrum with two sets of ^{13}C NMR resonances detected in the ranges of 220−235 and 260−270 ppm as well, as shown in Figure 5.

We suggest that these very low field signal sets are due to thioacetate moieties engaged in different coordination situations with the metal core of the cluster. To the best of our knowledge, there are no reports on the ^{13}C chemical shift values of the carbonyl moiety in thioacetate salts or thioacetate coordination compounds, likely because of the instability of this kind of subunit. Application of the Principal Component Analysis,[41] as developed by Tasic and Rittner,[42] allowed us to calculate for the (thio)-carbonyl ^{13}C nucleus a downfield shift of ca. 30 ppm on going from methyl acetate to methyl thioacetate. By applying this procedure to the zirconium oxo clusters recently published by some of us,[27a] where it is reported that the carbonyl ^{13}C nuclei of chelating acetates resonate at 184.7 ppm, we estimated for a chelating thioacetate a rough δ value of ca. 215 ppm, which is in acceptable agreement with the 220−235 ppm values found for the cluster. Moreover, in agreement with the literature,[43] we attribute the lowest-field $^1H-^{13}C$ (260−270 ppm) to the chelating thioacetates bearing a bridging carbonyl O atom observed in the crystal structure. This additional coordination should further deshield the ^{13}C nuclei and make the coordinative bond stronger. This is confirmed by the absence of exchange peaks in the phase-sensitive NOESY measurements (see Figure 1SM in the Supporting Information) between the ^1H nuclei of the corresponding methyl groups and those of the other methyl groups belonging to the chelating thioacetates, which, in contrast, exhibit intense exchange correlations, as was already found and discussed.[16d,45]

(41) Jackson, J. *A User's Guide to Principal Componets*; Wiley: New York, 1991.
(42) Tasic, L.; Rittner, R. *J. Mol. Struct.* **2009**, *33*, 15–19.
(43) Lin, S. J.; Hong, T. N.; Tung, J. N.; Chen, J. H. *Inorg. Chem.* **1997**, *36*, 3886.
(44) Faccini, F.; Fric, H.; Schubert, U.; Wendel, E.; Tsetsgee, O.; Müller, K.; Bertagnolli, H.; Venzo, A.; Gross, S. *J. Mater. Chem.* **2007**, *17*, 3297–3307.
(45) Perrin, C. L.; Dwyer, T. J. *Chem. Rev.* **1990**, *90*, 935–967.

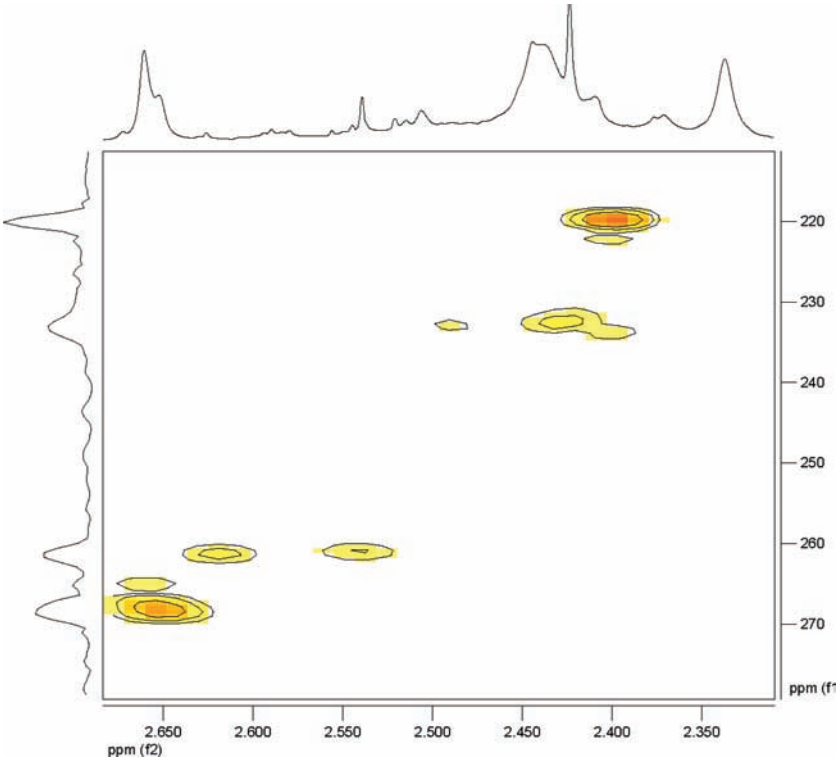

Figure 5. Portion of $^{1}H-^{13}C$ HMBC spectrum of $\mathbf{Zr_4}$.

4.4. Time-Resolved EXAFS Measurements. In order to achieve a deeper insight into the mechanism of the reaction of zirconium butoxide with monothioacetic acid in a 1:6 molar ratio, time-dependent EXAFS measurements were carried out during the first 20 h after the mixing of the two reactants. In Figure 6, the consecutive X-ray absorption near-edge structure (XANES) spectra are shown, together with $Zr(O^nBu)_4$ and $\mathbf{Zr_4}$ as references. Zirconium XANES spectra offer the possibility of gaining insight into the oxidation state by inspection of the edge position and the near coordination number around the X-ray absorber by inspection of the white line (first resonance after the edge step). As outlined in a previous work, Zr K-edge XANES spectra show a split white line for coordination numbers of 6 (octahedral) in the nearest-neighbor shells, while only a single resonance can be found for higher coordination numbers.[46] This is also evident in Figure 6. The reference spectrum of $Zr(O^nBu)_4$ shows the expected splitting because this compound is present as octahedrally coordinated dimeric species.[47] In contrast, the spectrum of $\mathbf{Zr_4}$, whose nearest-neighbor coordination is composed of five O and two S atoms, exhibits only a single white line. Although the white-line shape in the course of the reaction of zirconium butoxide with monothioacetic acid differs from the final product, only a single white line is still present over the whole period of 20 h; i.e., also these samples show a higher nearest-neighbor coordination number than 6. However, because of the rather broad white line, a mixture of six and higher coordinated zirconium centers is likely.

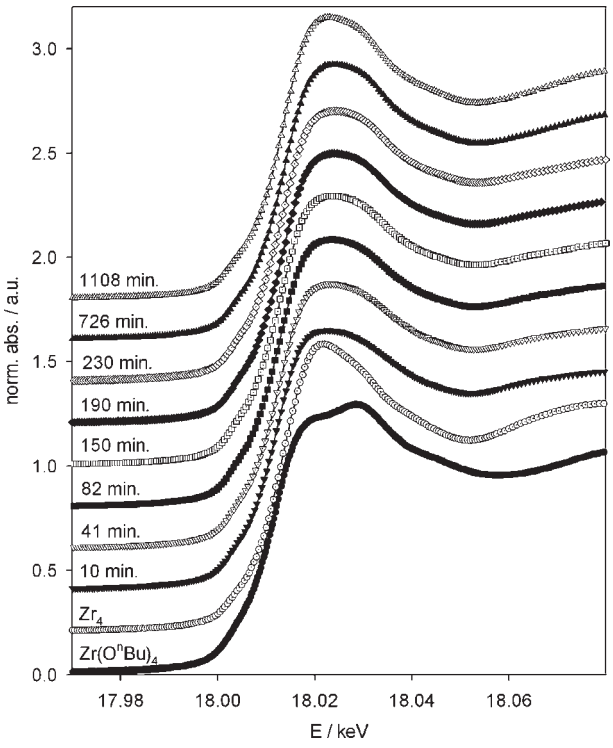

Figure 6. XANES spectra recorded for the references $Zr(O^nBu)_4$ and $\mathbf{Zr_4}$ and over the course of the reaction of $Zr(O^nBu)_4$ with 6 equiv of TAA at 278 K recorded at the times indicated in the graph. The spectra were shifted for clarity.

While the XANES analysis is restricted mostly to the nearest-neighbor coordination, evaluation of the EXAFS spectra, which are shown in Figure 7, allows more detailed insights into the reaction mechanism. The results of fitting of the experimental spectra with theoretical models

(46) Graziola, F.; Girardi, F.; Bauer, M.; Di Maggio, R.; Rovezzi, M.; Bertagnolli, H.; Sada, C.; Rossetto, G.; Gross, S. *Polymer* **2008**, *49*, 4332.
(47) Bauer, M.; Gastl, C.; Köppl, C.; Kickelbick, G.; Bertagnolli, H. *Monatsh. Chem.* **2006**, *137*, 567.

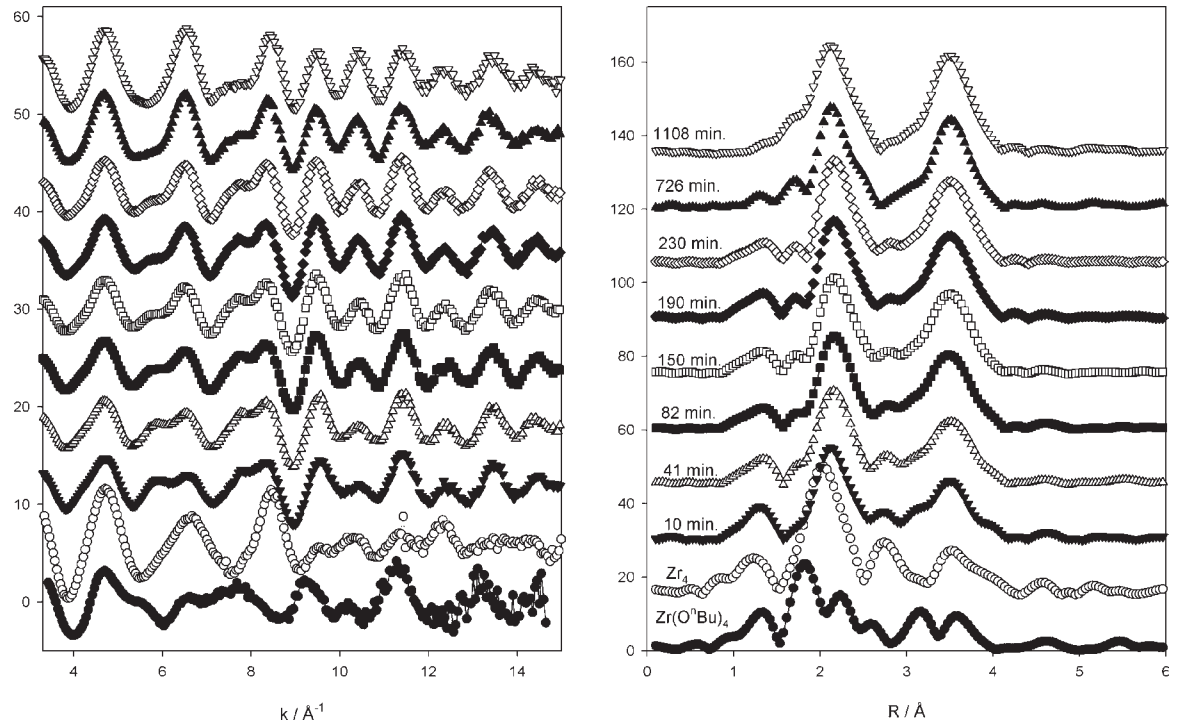

Figure 7. Experimental $k^3\chi(k)$ spectra (left) and their corresponding Fourier-transformed functions (left) of the references $Zr(O^nBu)_4$ and $\mathbf{Zr_4}$ also recorded over the course of the reaction of 1 mol of $Zr(O^nBu)_4$ with 6 mol of TAA at 278 K. The spectra were shifted for clarity.

are summarized in Table 6. The changes observed within the individual shells over the course of the reaction are summarized in Figure 8.

All spectra of the reaction were fitted with models consisting of Zr−O, Zr−S, and Zr−Zr contributions. Zr−C shells were not included in the first because of the problematic backscattering properties of carbon.[48] The first measurement was started approximately 10 min after mixing of the reactants; thus, the initial transformation of the starting compound $Zr(O^nBu)_4$ into an sulfur-containing species can be considered as rather fast. From Figure 7, it is evident that in the following time period the most significant changes in the $k^3\chi(k)$ spectra occur in the ranges 5−6, 7−8, and 10−11 $Å^{-1}$, while this is the case in the Fourier-transformed function between 2.5 and 3 and around 3.5 Å.

Fitting the spectra at the beginning required a short oxygen shell at around 1.9 Å, which is in very good agreement with the Zr−O1 shell found in $\mathbf{Zr_4}$. It has to be admitted that from the EXAFS data it is not clear whether a mixture of sulfur-containing species and $Zr(O^nBu)_4$ or only one complex with a short Zr−O1 contribution is present. However, because Zr−S and Zr−Zr contributions according to the final structure of the $\mathbf{Zr_4}$ cluster are already detected, the second case is more likely. However, over the course of the reaction, the short Zr−O1 contribution vanishes and only one Zr−O shell remains.

Although the coordination number of the second oxygen shell (Zr−O2) is higher than that in $\mathbf{Zr_4}$, its distance agrees quite well with the final cluster. The number of atoms remains rather constant until the shorter oxygen shell disappears. The overall oxygen coordination is slightly reduced from ~6 to 5 when only one Zr−O contribution can be found after 726 min but increases again to 6.7 after an additional 380 min, which can be considered as the first indication of another rearrangement.

Surprisingly, also a reduction of the Zr−S coordination number is observed in the first 20 h of the reaction from 0.7 to 0.1 and only a minor contribution remains at the end of the measurements. The sulfur shell at the beginning of the reaction is therefore more related to the final $\mathbf{Zr_4}$ cluster than that after 20 h. The Zr−Zr contributions show the opposite behavior because after 10 min the Zr−Zr1 coordination number is higher than that in the final $\mathbf{Zr_4}$ cluster and diminishes over the course of the reaction. The coordination number in the Zr−Zr2 shell is constantly slightly higher than that in $\mathbf{Zr_4}$, from which a more condensed cluster structure, likely a square pyramid or a tetrahedral cluster, can be deduced.[49]

From the EXAFS measurements, it is therefore clear that in the first 20 h of the reaction the final cluster is not yet formed (and actually its crystallization requires a longer time). Moreover, at the beginning, the shell structure of the final cluster is already present with shorter and longer Zr−O contributions, a Zr−S and two Zr−Zr shells, but this precluster structure of $\mathbf{Zr_4}$ is then subject to strong changes in the first 20 h of the reaction. At the end of the measurements, only the zirconium core exhibits a close relationship to $\mathbf{Zr_4}$, while the oxygen and sulfur shells indicate completely different structures in this time interval, which likely undergo further rearrangements and coordination/hydrolysis reactions to give the observed final structure.

(48) Bauer, M.; Müller, S.; Kickelbick, G.; Bertagnolli, H. *New J. Chem.* **2007**, *31*, **1950**.

(49) (a) Bauer, M.; Bertagnolli, H. *J. Phys. Chem. B* **2007**, *111*, 13756. (b) Bauer, M.; Bertagnolli, H. *Z. Phys. Chem.* **2009**, *23*, 877.

Table 6. Results from the Fitting of the Experimental EXAFS Spectra with Theoretical Models

sample	Abs−Bs[a]	N(Bs)[b]	R[c]/Å	σ[d]/Å	fit index[e]	E_f[f]/eV
$Zr(O^nBu)_4$	Zr−O1	1.8 ± 0.2	1.97 ± 0.02	0.032 ± 0.003		
	Zr−O2	1.4 ± 0.1	2.12 ± 0.02	0.022 ± 0.002		
	Zr−O3	2.0 ± 0.2	2.25 ± 0.02	0.045 ± 0.005		
	Zr−Zr	1.0 ± 0.3	3.55 ± 0.04	0.074 ± 0.022		
Zr_4	Zr−O1	*1*[g]	2.09 ± 0.02	0.032 ± 0.003	27.51	1.23
	Zr−O2	*4*[g]	2.22 ± 0.02	0.081 ± 0.008		
	Zr−S	*2.5*[g]	2.69 ± 0.02	0.112 ± 0.022		
	Zr−Zr1	*1*[g]	3.30 ± 0.03	0.102 ± 0.020		
	Zr−Zr2	*2*[g]	3.50 ± 0.04	0.092 ± 0.018		
After 10 min.	Zr−O	0.9 ± 0.1	1.93 ± 0.02	0.039 ± 0.004	31.24	−0.08
	Zr−O	5.1 ± 0.5	2.23 ± 0.02	0.084 ± 0.008		
	Zr−S	0.7 ± 0.1	2.72 ± 0.03	0.055 ± 0.006		
	Zr−Zr1	1.9 ± 0.4	3.28 ± 0.03	0.102 ± 0.020		
	Zr−Zr2	2.2 ± 0.4	3.48 ± 0.03	0.074 ± 0.015		
After 41 min.	Zr−O	0.9 ± 0.1	1.92 ± 0.02	*0.039*[h]	24.09	−0.92
	Zr−O	4.9 ± 0.5	2.24 ± 0.02	*0.084*		
	Zr−S	0.6 ± 0.1	2.74 ± 0.03	*0.055*		
	Zr−Zr1	1.5 ± 0.3	3.27 ± 0.03	*0.102*		
	Zr−Zr2	2.3 ± 0.4	3.49 ± 0.03	*0.074*		
After 82 min.	Zr−O	0.8 ± 0.1	1.93 ± 0.02	*0.039*	22.55	1.24
	Zr−O	4.9 ± 0.5	2.24 ± 0.02	*0.084*		
	Zr−S	0.5 ± 0.1	2.76 ± 0.03	*0.055*		
	Zr−Zr1	1.4 ± 0.3	3.25 ± 0.03	*0.102*		
	Zr−Zr2	2.5 ± 0.4	3.49 ± 0.03	*0.074*		
After 150 min.	Zr−O	0.8 ± 0.1	1.94 ± 0.02	*0.039*	22.23	−1.14
	Zr−O	5.1 ± 0.5	2.23 ± 0.02	*0.084*		
	Zr−S	0.5 ± 0.1	2.77 ± 0.03	*0.055*		
	Zr−Zr1	1.1 ± 0.2	3.26 ± 0.03	*0.102*		
	Zr−Zr2	2.6 ± 0.5	3.50 ± 0.04	*0.074*		
After 190 min.	Zr−O	0.7 ± 0.1	1.93 ± 0.02	*0.039*	22.91	−0.85
	Zr−O	5.3 ± 0.5	2.23 ± 0.02	*0.084*		
	Zr−S	0.4 ± 0.1	2.77 ± 0.03	*0.055*		
	Zr−Zr1	1.1 ± 0.2	3.26 ± 0.03	*0.102*		
	Zr−Zr2	2.7 ± 0.5	3.50 ± 0.03	*0.074*		
After 230 min.	Zr−O	0.7 ± 0.1	1.93 ± 0.02	*0.039*	21.88	−0.79
	Zr−O	5.4 ± 0.5	2.23 ± 0.02	*0.084*		
	Zr−S	0.4 ± 0.1	2.77 ± 0.03	*0.055*		
	Zr−Zr1	0.9 ± 0.2	3.26 ± 0.03	*0.102*		
	Zr−Zr2	2.6 ± 0.5	3.50 ± 0.03	*0.074*		
After 726 min.	Zr−O	5.6 ± 0.6	2.22 ± 0.02	0.084 ± 0.008	25.62	−0.65
	Zr−S	0.2 ± 0.1	2.76 ± 0.03	*0.055*		
	Zr−Zr1	0.3 ± 0.1	3.23 ± 0.03	*0.102*		
	Zr−Zr2	2.5 ± 0.5	3.51 ± 0.03	*0.074*		
After 1108 min.	Zr−O	6.7 ± 0.7	2.20 ± 0.02	0.092 ± 0.008	25.93	0.79
	Zr−S	0.1 ± 0.1	2.74 ± 0.03	*0.055*		
	Zr−Zr1	0.5 ± 0.1	3.20 ± 0.03	*0.102*		
	Zr−Zr2	2.8 ± 0.5	3.50 ± 0.03	*0.074*		

[a] Abs = X-ray-absorbing atom. Bs = backscatterer. [b] Number of backscattering atoms. [c] Distance between the X-ray absorber and the backscatterer. [d] Debye−Waller-like factor. [e] Quality of the fit. [f] Fermi energy, i.e., shift to account for discrepancies between the experimental and theoretical functions. [g] Values set to the crystallographic coordination numbers. [h] Set to the values of the sample after 10 min to ensure comparability.

4.5. Mechanistic Hypothesis for Cluster Formation. A particularly intriguing task in the investigation of these *thio* and *oxothio* clusters was to unravel the reaction steps leading to the formation of these polynuclear complexes starting from $Zr(O^nBu)_4$, which, according to recent EXAFS studies, evidenced in solution a dinuclear structure, with the Zr atoms in an octahedral coordination.[47,50]

The chemistry of monothioacetic acid, which is much more acidic (pK_a = 3.3) than the oxygen homologue acetic acid (pK_a = 4.76), is extensively reviewed in the literature.[51,17]

Thiocarboxylic acid undergoes tautomerism, with the thiol form (I) being the predominant one and, at lower temperature and in polar solvents, the thion form (II) prevailing (see Scheme 1SM in the Supporting Information).

The hydrolysis of monothioacetic acid to give acetic acid and hydrogen sulfide, according to the reactions shown in Scheme 2SM in the Supporting Information, has been thoroughly investigated by different authors[52] and the heat of hydrolysis has been determined, pointing out that the hydrolysis rate and the extent of conversion

(50) Bauer, M. Investigation of alkoxide precursor solutions and homogeneous catalyzed reactions by X-ray absorption and multi-dimensional spectroscopy. Ph.D. Thesis, Chemistry Faculty, University of Stuttgart, Stuttgart, Germany, 2008.

(51) (a) Ogawa, A.; Sonoda, N. *Comprehensive organic functional group transformation*; Katritzky, A. R., Meth-Cohn, O., Rees, C. W., Eds.; Pergamon: Oxford, England, 1995; Vol. *5*, p 231. (b) Rajab, M. A.; Noe, E. A. *J. Am. Chem. Soc*. **1990**, *112*, 4697–4700.

(52) (a) Sunner, S.; Wadsö, I. *Trans. Faraday Soc*. **1957**, *53*, 445. (b) Hipkin, J.; Satchell, D. P. N. *Tetrahedron* **1965**, *21*, 835–842. (c) Edward, J. T.; Welch, G.; Wong, S. C. *Can. J. Chem*. **1978**, *56*, 935–940.

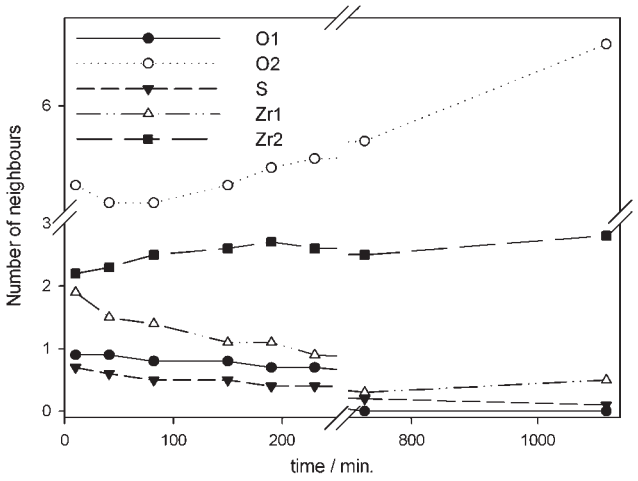

Figure 8. Summary of the kinetic changes in the individual neighbor shells over the course of the reaction according to Table 6.

to acetic acid are both enhanced by acidic media and low pH.[52b]

In the reactions described in this paper, monothioacetic acid can interact both with the coordinated ^{n}BuO moiety of $Zr(O^{n}Bu)_4$ as well as with ^{n}BuOH coordinated to the alkoxide in the commercial formulation. It also needs to be taken into account that in most of our reactions monothioacetic acid is employed in a large excess. The esterification reaction between the alcohol and monothioacetic acid generates H_2O, which can be considered the starting reagent for a large series of reactions. In fact, on the basis of the experimental evidence (development of H_2S) and literature data,[53] it is reasonable to consider the following side reactions, which account for the formation of both acetic and dithioacetic acids whose anions are present in two of our clusters. The plethora of described reactions and equilibria (tautomerism and hydrolysis of monothioacetic acid, hydrolysis and condensation, coordination, rearrangements), often simultaneously occurring in the reaction batch, and the lack of analytical tools to reliably follow these processes dramatically complicates the picture. As described at the beginning of the Results and Discussion section, different experiments were carried out to try to elucidate the reaction sequence, and on the basis of the obtained results and of previous knowledge, some "mechanistic" hypothesis for the formation of the different species can be proposed.

Concerning the **Zr$_4$** cluster, characterized by the S,O μ coordination of thiocarboxylate ligands, where O is bridging and S coordinates to the metal, it is reasonable to assume that its formation proceeds along the reaction pattern similar to that already proposed[25,27b] for the homologous oxo clusters (see Scheme 1).

The above scheme accounts also for the presence of μ_3-O, found in both **Zr$_4$** and **Zr$_6$**, and of the acetate anion, found in **Zr$_6$**. As far as this last point is concerned, even though we have no experimental evidence, it has to be highlighted that the acetate ion is present only in **Zr$_6$**. This finding is in agreement with the fact that the formation of **Zr$_6$** seems to occur in a second step, after the formation of **Zr$_4$**. Actually, time-resolved EXAFS data suggest that,

(53) Iwahori, K.; Yamashita, I. *J. Phys.* (*Paris*) **2007**, *61*, 492.

Scheme 1. Possible Reaction Patterns for the Formation of Oxo and Oxothio Clusters

Substitution

$$Zr(OBu)_4 + CH_3COSH \rightleftharpoons Zr(OBu)_{4-n}-(CH_3COS) + n\ BuOH$$

Reactions with alcohol

$$BuOH + CH_3COSH \rightleftharpoons CH_3COOBu + H_2S \qquad \textbf{2.a}$$

$$BuOH + CH_3COOH \rightleftharpoons CH_3COOBu + H_2O \qquad \textbf{2.b}$$

$$BuOH + CH_3CSSH \rightleftharpoons CH_3CSOBu + H_2S \qquad \textbf{2.c}$$

Condensation

$$Zr(OBu)_{4-n}-(CH_3COS) + H_2X \rightleftharpoons Zr_aX_b(OR)_c(CH_3COS)_n$$

X = O, S

after a first fast coordination of monothioacetate, a complex sequence of events, likely involving also one or more rearrangements of the first formed structure, occur. These rearrangements would account for the formation of a more complex (and quite unusual) structure than that observed in **Zr$_6$**, in which the structural motifs are similar to those observed in **Zr$_4$**, as explained below.

Moreover, Scheme 1 and equilibria shown in Schemes 1SM and 2SM in the Supporting Information account also for the evolution of H_2S, which develops in the first stages of the reaction, and it is assumed to be a key step for the formation of the other structure observed, **Zr$_3$**.

In fact, in the thiocluster **Zr$_3$**, it is possible to observe the presence only of sulfur-based ligands, actually dithioacetates and the peculiar ethane-1,1,1-trithiolate moiety, $[\mu_3\text{-}S_3CCH_3]^{3-}$. While the formation of dithioacetate ions is related to the equilibrium (1b) of Scheme 2SM in the Supporting Information, the presence of the $[\mu_3\text{-}S_3CCH_3]^{3-}$ trianion is more complicated to explain, even though the participation of H_2S or S^{2-} in its formation seems evident.

It was worth noting that the ethane-1,1,1-trithiolate moiety has been previously found as a ligand in a nickel(II) cluster obtained by Bonamico et al.[40] by the reaction of nickel bis(dithioacetate) with CS_2, whereas Kniep and Reski[54] reported the formation of a 1:1 adduct of AsI_3 with hexathiaadamantane (shown in Figure 9) by the reaction of AsI_3 with monothioacetic acid. This hexathiaadamantane group was also obtained by the reaction of monothioacetic acid with $ZnCl_2$, as reported by Stetter.[55]

Although it was not possible, on the basis of the available experimental evidences, to propose a complete mechanism for the formation of this unusual $\mu_3\text{-}S_3CCH_3$ ligand, it is reasonable to assume that the species $CH_3CS_2^-$ and S^{2-} are involved.

(54) Kniep, R.; Reski, H. D. *Inorg. Chim. Acta* **1982**, *64*, L83–L84.
(55) Stetter, H. *Angew. Chem.* **1954**, *66*, 217.

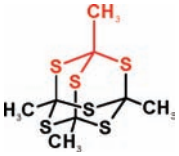

Figure 9. Hexathiaadamantane obtained by the reaction of TAA with AsI_3, by Kniep and Reski.[54]

Scheme 2. Reaction Conditions Leading to the Formation of $\mathbf{Zr_4}$, $\mathbf{Zr_6}$, and $\mathbf{Zr_3}$

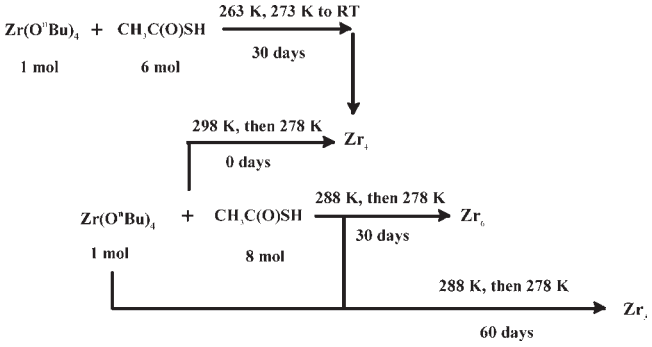

It can be argued that, in the presence of these species, a first cluster structure with sulfide ligands forms to which, in a second step, the dithioacetate ligands attach. This hypothesis seems to be strengthened by the experimental evidence that the formation of $\mathbf{Zr_3}$ requires longer time, after the formation of $\mathbf{Zr_4}$ (first obtained product) and $\mathbf{Zr_6}$ (second product), i.e., after that extended hydrolysis reaction occurred, with the formation of H_2S. Moreover, it has also to be highlighted that whenever H_2S was added as a coreactant to the reaction mixture the selective formation of $\mathbf{Zr_3}$ was observed, thus confirming that S^{2-} is actually involved in the formation of this thiocluster. The relevance of hydrolytic processes in the formation of the reported zirconium clusters is strengthened by the experimental evidence that the crystals of $\mathbf{Zr_4}$ are formed *before* those of $\mathbf{Zr_6}$, whose formation requires the occurrence of complete hydrolysis reaction.

Finally, the hexanuclear structure of $\mathbf{Zr_6}$ has never been observed before. Its formation can be explained by assuming the aggregation of dimeric and trimeric units (analogues to those leading to the formation of $\mathbf{Zr_4}$), in the presence of acetic acid in the reaction mixture. By considering the structure of $\mathbf{Zr_6}$, it is possible to evidence the presence of a repeating structural unit, observed also in the $\mathbf{Zr_4}$ structure, thus strengthening the assumption of the preliminary formation of the structural units leading to $\mathbf{Zr_4}$, which presents exclusively monothioacetate ligands and which, under suitable conditions, can rearrange to give $\mathbf{Zr_6}$. The complete reaction patterns are sketched in Scheme 2.

5. Conclusions

The reaction of zirconium butoxide with monothioacetic acid resulted in three crystalline polynuclear complexes, which are characterized by different cluster cores and different sulfur-containing and sulfur-free ligands. The clusters evidence that the reactions in this system are by far more complex than the corresponding reactions with carboxylic acids because of the simultaneous equilibria of the precursor acid.

In particular, the presence of coexisting equilibria of monothioacetic acid, leading to the formation of H_2S and of the dithioacetate species strongly affects the occurrence of the reactions and the nature of the final product. In fact, two of the formed clusters ($\mathbf{Zr_4}$ and $\mathbf{Zr_6}$) are characterized by the S,O μ-coordination of thiocarboxylate ligands, and it is reasonable to assume that their formation occurs following a reaction pattern similar to that already observed in the case of oxo clusters.

On the contrary, as far as the thiocluster $\mathbf{Zr_3}$ is concerned, which is characterized by the presence of only sulfur-based ligands (dithioacetates and the peculiar ethane-1,1,1-trithiolate moiety, $[\mu_3\text{-}S_3CCH_3]^{3-}$), a completely different reaction pattern is expected to take place. In this case, the involvement of H_2S or S^{2-} [either free or coordinated *to* (and activated *by*) the metal atom] to its formation could be argued. These species would lead to the formation of a first cluster structure based only on sulfide ligands to which the dithioacetate ligands formed by hydrolysis of monothioacetic acid coordinate in a second step. Accordingly, the formation of this thiocluster requires more time (necessary for the extended hydrolysis reaction, leading to the release of H_2S), and it is favored in the presence of an excess of H_2S in the reaction batch.

It might be interesting, in this regard, to compare the relatively well-known and established oxo cluster chemistry with these new thioxo and dithio clusters. Apart from the already highlighted analogies in coordination modes, nuclearities, and polyhedra arrangements and connectivities, there are also remarkable differences.

First of all, the most striking difference, which can be traced back by the "hybrid" nature of the chosen ligand, bearing both sulfido and oxo teeth, is the presence of concurring equilibria, involving monothioacetic acid and accounting for the presence in solution of monothio- and dithioacetate species which could all be detected in the three different structures, as well as the presence of both sulfido and oxo bridges. In the homologue oxo clusters the ligands, both chelating and bridging, are in all cases carboxylates, and the bridges are mainly oxo or hydroxo ions.

The manifold nature of the species present in solution remarkably complicates the overall picture, thus making particularly difficult to propose a reaction mechanism. The only conclusions we can draw in that regard are summarized in Schemes 1 and 2.

In conclusion, the described thio and oxothio clusters evidence as the well-established chemistry of the homologous oxo clusters (based on O−M−O bonds) can actually be extended to the sulfur-based species, and polynuclear clusters in which both S−M−O and S−M−S bridges are present can be obtained. However, it should be pointed out that, in this case, the existence of different equilibria involving the bidentate ligand remarkably affects the fate of the reaction, leading to the formation of species completely different from the structural and coordination points of view with respect to those observed in the case of the oxo clusters. Indeed, although some recurring structural motifs are similar to those observed in the case of oxo clusters, such as the presence of chelating and bridging modes for the bidentate (thio- and dithioacetate) ligands, completely new coordination fashions and geometries are observed.

On the basis of these considerations, it can be highlighted that the presented results, although several questions and chemical issues still remain open, pave the way for the investigation of a still relatively unexplored field of research, i.e., the polynuclear chemistry of early transition metals with sulfido and oxo/sulfido ligands. The obtained results and structures contribute to shedding light on the already outlined complex chemistry of these systems and also to triggering new research on further metals such as hafnium, titanium, and vanadium as well as on further ligands (e.g., dithioacetic acid, thiomethacrylic acid, etc.),

Acknowledgment. The Italian National Research Council (CNR), the University of Padova, the Italian Consortium INSTM, and the Austrian Science Funds (FWF), Wien, Austria (Project P19199), are acknowledged for providing money and equipment. We thank the Deutsches Elektronen Synchrothron (DESY) and the European Community for financial support in activities at Hasylab, DESY: the research leading to these results has received funding from the European Community's Seventh Framework Program (FP7/2007-2013) under Grant 226716. Matthias Abele and Christoph Gastl are gratefully acknowledged for their skillful support.

Supporting Information Available: Experimental details, schemes of the tautomeric equilibrium between the thiol (I) and thion (II) forms of TAA and hydrolysis reactions of monothioacetic acid, and a figure showing a portion of the phase-sensitive NOESY spectrum of $\mathbf{Zr_4}$. This material is available free of charge via the Internet at http://pubs.acs.org.

Note Added after ASAP Publication. This paper was published on the Web on December 9, 2010. References 2 and 31b were updated, and the corrected version was reposted on December 15, 2010.